

# Magnetically Separable Fe<sub>3</sub>O<sub>4</sub>/SnO<sub>2</sub>/Graphene Adsorbent for Waste Water Removal

V Paramarta<sup>1,2</sup>, A Taufik<sup>1,2</sup> and R Saleh<sup>1,2</sup>

<sup>1</sup>Departemen Fisika, Fakultas MIPA (Department of Physics, Faculty of Mathematics and Natural Sciences)-Universitas Indonesia, 16424 Depok, Indonesia

<sup>2</sup>Integrated Laboratory of Energy and Environment, Fakultas MIPA-Universitas Indonesia, 16424 Depok, Indonesia

Email: rosari.saleh@gmail.com

**Abstract.** Our previous study conducted the SnO<sub>2</sub> and SnO<sub>2</sub>/graphene adsorption efficiency in Methylene Blue removal from aqueous solution, however, the difficulty of adsorbent separation from the methylene blue solution limits its efficiency. Therefore, in this work, SnO<sub>2</sub> and SnO<sub>2</sub>/graphene was combined with Fe<sub>3</sub>O<sub>4</sub> to improve the separation process and adsorption performance for removing the organic dyes. Fe<sub>3</sub>O<sub>4</sub>/SnO<sub>2</sub>/grapheme were synthesized by using the co-precipitation method. The graphene content was varied from 1, 3, and 5 weight percent (wt%). The crystalline phase and thermal stability of the samples were characterized by using X- ray Diffraction (XRD) and Thermal Gravimetric Analysis (TGA). The adsorption ability of the samples was investigated by using significant adsorption degradation of MB observed when the graphene in Fe<sub>3</sub>O<sub>4</sub>/SnO<sub>2</sub> nanocomposite was added. The other parameters such as pH and initial concentration have also been investigated. The reusability was also investigated to study the stability of the samples. The fitting of equilibrium adsorption capacity result indicates that the adsorption mechanism of Fe<sub>3</sub>O<sub>4</sub>/SnO<sub>2</sub> nanocomposite with graphene tends to follow the Langmuir adsorption isotherm model.

**Keywords:** SnO<sub>2</sub>, Fe<sub>3</sub>O<sub>4</sub>/SnO<sub>2</sub>, graphene, adsorption, methylene blue.

## 1. Introduction

The environmental pollution has increased public concern nowadays because of its problem for aquatic life and environment. This problem must be decreased by using the suitable methods and technologies [1]. Methylene blue (MB) dye is one of the cationic dyes used as a material for dyeing wood, cotton, and silk [2]. A variety of methods such as adsorption, coagulation and flocculation, oxidation, chemical precipitation, and so forth, have been reported for wastewater treatment [3]. Among these, adsorption is an attractive and favorable technique because of their high efficiency, cost effectiveness, and simple operation [4].

A variety of sorbents have been tested to remove dyes in aqueous solution, and some metal oxides exhibit prominent potentials for adsorptive removal of dye waste [5]. One of metal oxide that is widely used in the degradation process of dye wastes is a tin oxide (SnO<sub>2</sub>). SnO<sub>2</sub> has various advantages such as its sensitivity when it is exposed to the light and thermal energy, its numbers of an intrinsic defect in its structure caused by low formation energy and strong attraction between the tin sites and oxygen



vacancies [6]. Graphene, a novel one-atom-thick two-dimensional graphitic carbon system with sp<sup>2</sup>-bonded carbon localized on the honeycomb lattice, has been under intense multidisciplinary study attribute to its extraordinary electrical and mechanical properties, large surface area, an excellent mobility of charge carriers, and good thermal conductivity [7]. Furthermore, combining the graphene material into the metal oxide can enhance the adsorption performance of the sample due to their functional groups and defect sites of graphene extending the lifetime of the adsorbent material by acting as support material which inhibits leaching of fine metal oxide nanoparticles into the treated water [8]. The coupling SnO<sub>2</sub> and graphene with magnetic adsorbent were investigated widely to overcome the disadvantage for difficult separation. Several researchers have reported on the use of Fe<sub>3</sub>O<sub>4</sub> for removal and separation of dyes [9-10]. Therefore, it is believed that combining SnO<sub>2</sub>, Fe<sub>3</sub>O<sub>4</sub> and graphene will exhibit excellent adsorptive with highly effectively recovery by magnetic separation technique.

In this study, Fe<sub>3</sub>O<sub>4</sub>/SnO<sub>2</sub> nanoparticle will be combined with various weight percentages of graphene (1, 3, and 5 wt%) that are applied as adsorbents to degrade the methylene blue (MB) dye and the adsorption mechanism, pH, initial concentration, and temperature of these composites. The sample was characterized by using X-ray Diffraction (XRD) and Thermal Gravimetric Analysis (TGA).

## 2. Experimental Method

### 2.1 Chemicals

All reagents used were analytical grade without further purification. Anhydrous tin chloride (SnCl<sub>2</sub>), iron (II) sulfate heptahydrate (FeSO<sub>4</sub>·7H<sub>2</sub>O), sodium hydroxide (NaOH), methylene blue (MB), ethanol, ethylene glycol (EG) were purchased from Merck (Kenilworth, NJ, USA). Graphene was bought from Angstrom Material.

### 2.2 Preparation of SnO<sub>2</sub> nanoparticle and Fe<sub>3</sub>O<sub>4</sub>/SnO<sub>2</sub> nanocomposites

The Fe<sub>3</sub>O<sub>4</sub> nanoparticles were synthesized by using the same method used in our previous study [11]. The SnO<sub>2</sub> nanoparticles were synthesized by using a modification of the method reported by Yue Li and co-workers [12]. First, SnCl<sub>2</sub> was dissolved in a mixture of ethanol and aqueous solution, which was then added into the NaOH solutions by using magnetic stirrer. Then, the mixed solutions were heated at 180 °C for 3 h, then chilled to room temperature. The precipitate was obtained by centrifugation and washed by using aqueous solutions and ethanol several times. The precipitated particles were dried under vacuum at 80 °C, and SnO<sub>2</sub> particles obtained by calcination for 3 h at 700 °C. The Fe<sub>3</sub>O<sub>4</sub>/SnO<sub>2</sub> nanocomposites were synthesized by using the sol-gel method. First, SnO<sub>2</sub> nanoparticles were mixed with Fe<sub>3</sub>O<sub>4</sub> in a mixture of ethanol and aqueous solution. Each mixture was ultrasonicated for 2 h and then centrifuged to obtain the precipitate. The resulting product was then dried under vacuum at 80 °C for 12 h to obtain Fe<sub>3</sub>O<sub>4</sub>/SnO<sub>2</sub> nanocomposites.

### 2.3 Preparation of Fe<sub>3</sub>O<sub>4</sub>/SnO<sub>2</sub>/graphene composites

Fe<sub>3</sub>O<sub>4</sub>/SnO<sub>2</sub>/graphene was synthesized by using the co-precipitation method. First, graphene with various weight percentage (1, 3, 5 wt%) was dissolved in distilled water and ethanol through the ultrasonic treatment for 2 hours, then Fe<sub>3</sub>O<sub>4</sub>/SnO<sub>2</sub> nanocomposites were poured into the solution and stirred magnetically. The mixed solution was then heated at 120 °C for 3 hours. The result of a solution was then centrifuged and dried at 70 °C under vacuum condition.

### 2.4 Characterization

The sample was characterized by XRD using a Rigaku Miniflex 600 (Rigaku, Tokyo, Japan) with a Cu K- $\alpha$  radiation source ( $\lambda = 1.5406 \text{ \AA}$ ) and thermal gravimetric analysis (TGA) of the sample obtained by using Rigaku TG8121 with the temperature from 27 °C until 900 °C.

### 2.5 Adsorption processes

Adsorption experiment was carried out by mixing Fe<sub>3</sub>O<sub>4</sub>/SnO<sub>2</sub>/graphene into methylene blue (MB) solution used as pollutant model with the concentration of 20 mg/L, and the pH solution was adjusted By using NaOH. The concentration of dye was analyzed by using UV-Vis Spectrometer. The maximum degradation and the amount of MB adsorbed onto sample were calculated by using the following equation:

$$\text{Maximum degradation (\%)} = (C_t - C_0) \times 100\% / C_0 \quad (1)$$

$$q_t = (C_0 - C_t)V/W; q_e = (C_0 - C_e) V/m \quad (2)$$

where C<sub>0</sub> and C<sub>t</sub> (mg L<sup>-1</sup>) are initial and real-time concentration of organic pollutant, respectively. q<sub>t</sub> (mg g<sup>-1</sup>) is the amount of adsorbed per unit mass of the absorbent at time t. V (L) is the volume of the absorbed solution and m (g) is the mass of the absorbent. Furthermore, adsorption experiment is carried out again by varying MB concentration for sample with best adsorption activity.

### 3. Results and Discussion

The crystalline structure of the Fe<sub>3</sub>O<sub>4</sub>/SnO<sub>2</sub>/graphene composite with various weight percentages (1, 3, 5 wt% labeled as FS-g 1wt%, FS-g 2wt% and FS-g 5wt%, respectively) were analyzed by XRD and showed in Fig. 1. All of the Fe<sub>3</sub>O<sub>4</sub>/SnO<sub>2</sub>/graphene composites displayed peaks corresponding to the tetragonal structure of SnO<sub>2</sub> and cubic spinel structure from Fe<sub>3</sub>O<sub>4</sub>. In Fig. 1, the diffraction peaks at 2θ = 26.5°, 33.8°, 38°, 39°, 51.8°, 54.8°, 58°, 62°, 64.7°, 65.8°, 71.2°, 78.2°, 81.2°, 83.7° were assigned to the characteristic peak of SnO<sub>2</sub>, which corresponded to the crystal planes of (110), (101), (200), (111), (211), (220), (002), (310), (112), (301), (202), (321), (400), and (222), respectively. The diffraction pattern of Fe<sub>3</sub>O<sub>4</sub> was observed at the value of 2θ = 30.14°, 35.49°, 43.28°, 57.20°, 62.83°, and 74.8° corresponding to each area (220), (311), (400), (511), (440) and (533), respectively. For graphene, there is only a broad peak at around of 2θ of 25°, which shows the amorphous structure of graphene. As can be seen, the diffraction peak of the SnO<sub>2</sub> and graphene were overlapped at 2θ around 26° at Fe<sub>3</sub>O<sub>4</sub>/SnO<sub>2</sub>/graphene composites.

Figure 2 shows the weight loss curve for Fe<sub>3</sub>O<sub>4</sub>/SnO<sub>2</sub>/graphene composites with different weight percentages (1, 3, and 5 wt%) obtained from TGA measurement. As can be seen, Fe<sub>3</sub>O<sub>4</sub>/SnO<sub>2</sub> nanoparticle did not exhibit the significant percentage loss in the result of TGA measurement which indicated that Fe<sub>3</sub>O<sub>4</sub>/SnO<sub>2</sub> nanoparticle without any addition of graphene was stable until 1000°C. The weight loss started around 100°C was due to the volatilization of adsorbed water [13]. The weight loss stage from 400°C decomposition took place thereafter [14]. The percentage loss of the samples could be identified as the total amount of graphene in the samples. Furthermore, the weight loss of graphene at TGA measurement could confirm the existence of the graphene in Fe<sub>3</sub>O<sub>4</sub>/SnO<sub>2</sub>/graphene composite samples.

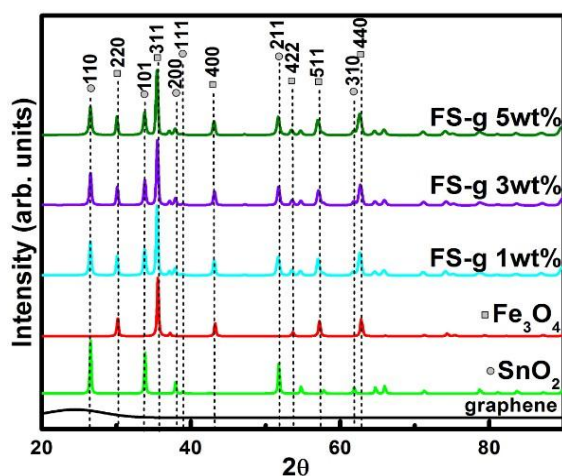


**Figure 1.** XRD patterns of  $\text{Fe}_3\text{O}_4/\text{SnO}_2$  nanocomposite and  $\text{Fe}_3\text{O}_4/\text{SnO}_2/\text{graphene}$  with various weight percentages (1, 3, 5 wt%)

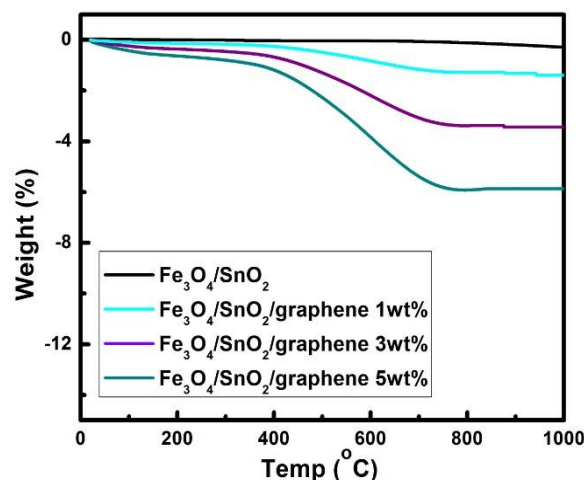


**Figure 2.** TGA curve of  $\text{Fe}_3\text{O}_4/\text{SnO}_2$  nanocomposite and  $\text{Fe}_3\text{O}_4/\text{SnO}_2/\text{graphene}$  with various weight percentages (1, 3, 5 wt%)

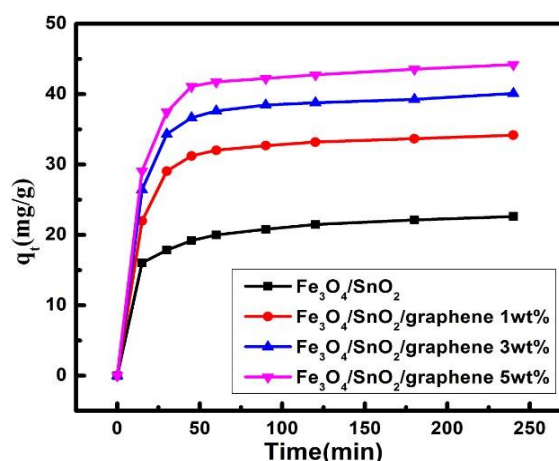
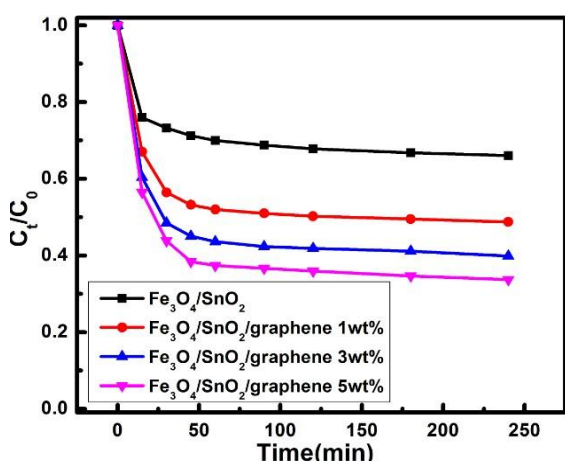


**Figure 3.** (a) Decolorization process of MB concentration and (b) adsorption capacity of  $\text{Fe}_3\text{O}_4/\text{SnO}_2/\text{graphene}$  5 wt%

Figure 3 shows the adsorption ability of the  $\text{Fe}_3\text{O}_4/\text{SnO}_2/\text{graphene}$  composites with various weight percentages (1, 3, and 5 wt%). The results show that  $\text{Fe}_3\text{O}_4/\text{SnO}_2/\text{graphene}$  5 wt% composites exhibited the highest adsorption ability than  $\text{Fe}_3\text{O}_4/\text{SnO}_2/\text{graphene}$  of 1 wt%,  $\text{Fe}_3\text{O}_4/\text{SnO}_2/\text{graphene}$  of 3 wt%, and  $\text{Fe}_3\text{O}_4/\text{SnO}_2$  composite. Fig. 3a shows the color change (decolorization) of MB during the adsorption process. The decolorization process increased simultaneously with the addition of weight percentage of graphene at  $\text{Fe}_3\text{O}_4/\text{SnO}_2$  from 33.94% for  $\text{Fe}_3\text{O}_4/\text{SnO}_2$  nanoparticle until 51.25%, 60.13%, and 66.29% for  $\text{Fe}_3\text{O}_4/\text{SnO}_2/\text{graphene}$  of 1, 3, 5 wt%, respectively. The certain contact time during an adsorption process was performed to identify the adsorption capability of the adsorbent to adsorb the pollutants on its surface per unit of time [15]. Fig. 3b shows the adsorption capacity against time up to 250 minutes. As can be seen in Fig. 3b,  $\text{Fe}_3\text{O}_4/\text{SnO}_2/\text{graphene}$  5 wt% showed the highest adsorption capacity (44.19 mg/g) then followed by  $\text{Fe}_3\text{O}_4/\text{SnO}_2/\text{graphene}$  3 wt% (40.08 mg/g),  $\text{Fe}_3\text{O}_4/\text{SnO}_2/\text{graphene}$  1 wt% (34.16 mg/g) and  $\text{Fe}_3\text{O}_4/\text{SnO}_2$  (22.62 mg/g). The maximum adsorption capacity of the samples reached at amount graphene material in  $\text{Fe}_3\text{O}_4/\text{SnO}_2/\text{graphene}$  was 5 wt%. It may due to the increase of the surface area because the addition of graphene was proportional to the mass of graphene in the solution [16].

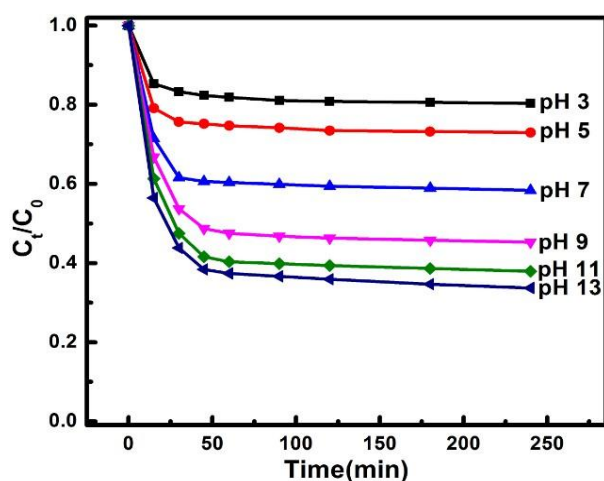


**Figure 4.** Effect of pH in adsorption capacity of  $\text{Fe}_3\text{O}_4/\text{SnO}_2/\text{graphene}$  of 5 wt%

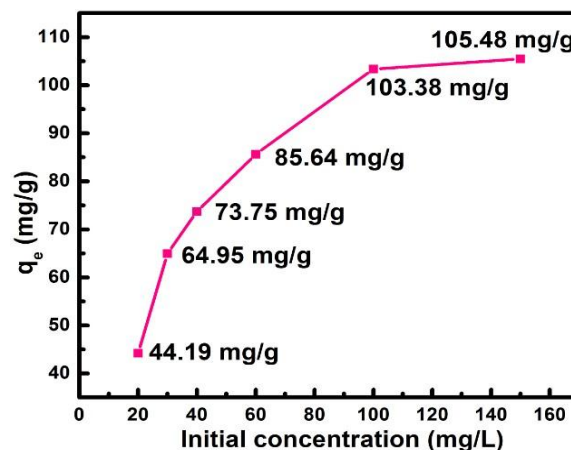


**Figure 5.** Adsorption capacity of  $\text{Fe}_3\text{O}_4/\text{SnO}_2/\text{graphene}$  of 5 wt% with different MB concentration

Figure 4 shows the influence of pH in the adsorption ability of  $\text{Fe}_3\text{O}_4/\text{SnO}_2/\text{graphene}$  of 5 wt% with broad range of pH from pH 3 until pH 13. All measurements were made at room temperature and for the contact time of 4 hours. The result showed the adsorption ability was found to increase with the increasing solution pH. The lower value of adsorption ability at acidic pH may be due to the presence of excess  $\text{H}^+$  ions from the acid solution competing with the charge MB dye cations for vacant adsorption site [3,17]. That phenomenon indicated the maximum adsorption capacity was obtained at the pH value of 13 for  $\text{Fe}_3\text{O}_4/\text{SnO}_2/\text{graphene}$  5 wt% composite.

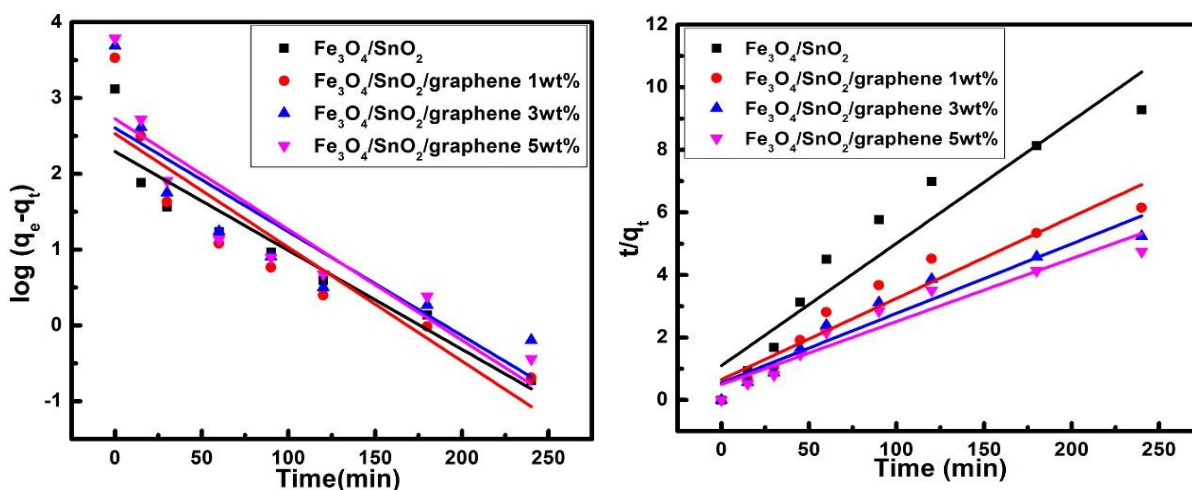


**Figure 6.** (a) Pseudo-first-order and (b) Pseudo-second-order plots for MB adsorption of  $\text{Fe}_3\text{O}_4/\text{SnO}_2$  nanocomposite and  $\text{Fe}_3\text{O}_4/\text{SnO}_2/\text{graphene}$  with various weight percentages (1, 3, 5 wt%)

To investigate the influence of the initial concentration of MB dye, Figure 5 shows the adsorption capacity of  $\text{Fe}_3\text{O}_4/\text{SnO}_2/\text{graphene}$  of 5 wt% composite with the variation of MB concentration from 20 mg/L– 150 mg/L with the adsorbent dosage of 0.3 g/L. The result shows, the adsorption capacity of  $\text{Fe}_3\text{O}_4/\text{SnO}_2/\text{graphene}$  decreased with the increase of MB concentration with the equilibrium adsorption capacity reach its maximum of 105.48 mg/g.

The pseudo-first-order (Figure 6a) and pseudo- second-order (Figure 6b) models were examined in this study to analyze the kinetics of MB adsorption. The selection of the best applicable adsorption kinetics model for the adsorption of MB onto the samples was done on the basis of the values of the

correlation ( $R^2$ ). The pseudo first-order model can be expressed as follows:

$$\text{Log}(q_e - q_t) = \log q_e - (k_1/2.303)t \quad (3)$$

where  $q_e$  and  $q_t$  are the adsorption capacity of  $\text{Fe}_3\text{O}_4/\text{SnO}_2$  nanocomposite and  $\text{Fe}_3\text{O}_4/\text{SnO}_2/\text{graphene}$  with various weight percentages (1, 3, 5 wt%) for MB at equilibrium ( $\text{mg g}^{-1}$ ) and at given time (min), respectively. While  $k_1$  is the rate constant for the pseudo-first-order of the adsorption ( $\text{g mg}^{-1} \text{min}^{-1}$ ).

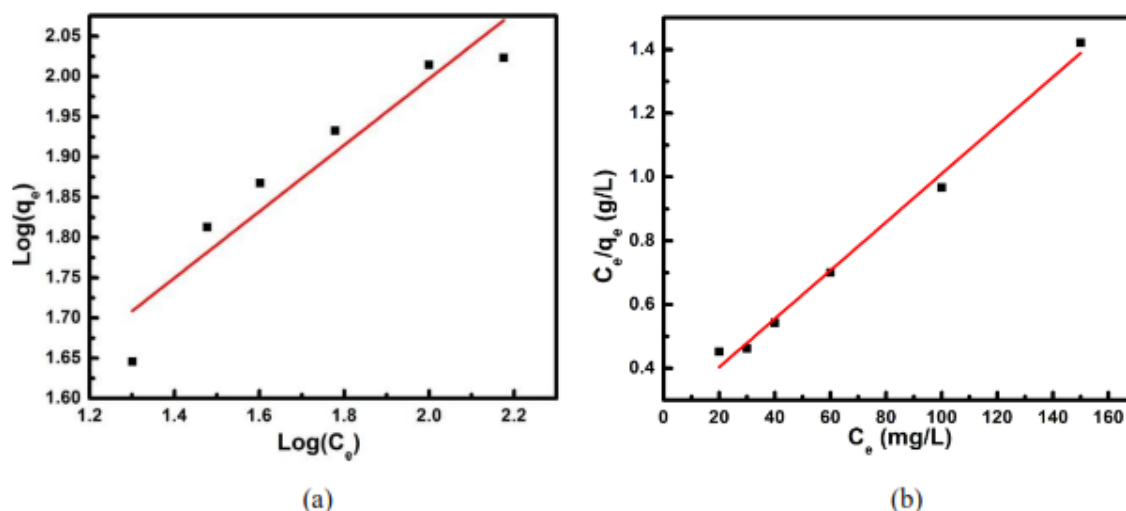


**Figure 7.** (a) Freundlich and (b) Langmuir adsorption-isotherm model fitting the experimental data of  $\text{Fe}_3\text{O}_4/\text{SnO}_2/\text{graphene}$  of 5 wt%

**Table 1.** Kinetic parameter of the pseudo-first-order and pseudo-second-order models for the adsorption of MB onto  $\text{Fe}_3\text{O}_4/\text{SnO}_2$  nanocomposite and  $\text{Fe}_3\text{O}_4/\text{SnO}_2/\text{graphene}$  with various weight percentages (1, 3, 5 wt%)

Sample	$q_e$ (mg/g) exp	The pseudo-First-order rate			The pseudo-second-order rate		
		$q_{1e}$ (mg/g)	$K_1$	$R^2$	$q_{2e}$ (mg/g)	$K_2$	$R^2$
$\text{Fe}_3\text{O}_4/\text{SO}_2$	22.629	9.921	0.013	0.875	25.555	0.0013	0.90121
$\text{Fe}_3\text{O}_4/\text{SnO}_2/\text{graphene}$ 1 wt%	34.168	12.549	0.015	0.823	38.491	0.0010	0.9189
$\text{Fe}_3\text{O}_4/\text{SnO}_2/\text{graphene}$ 3 wt%	40.088	1.002	0.013	0.760	44.984	0.0008	0.91867
$\text{Fe}_3\text{O}_4/\text{SnO}_2/\text{graphene}$ 5 wt%	44.196	15.260	0.014	0.786	49.652	0.0008	0.91894

The pseudo-second-order model, can be expressed as follows:

$$t/q_t = 1/(k_2 \cdot q_e^2) + t/q_e \quad (4)$$

where  $k_2$  is the rate constant for the pseudo-second-order adsorption process [4]. The value of the  $R^2$  for the pseudo-first-order and pseudo-second-order models are shown in Table 1. The low value of the correlation coefficient  $R^2$  indicated that the adsorption of MB onto samples poorly fitted with pseudo first-order kinetic model. However, the adsorption of MB onto all samples shows a better fit to the correlation coefficient  $R^2$  of the pseudo-second-order model. That case indicated the adsorption process were confirmed to the pseudo-second-order kinetics. Two adsorption kinetics models were applied to know the mechanism of the adsorption process. Figure 7 shows the Freundlich (Figure 7a) and Langmuir (Figure 7b) adsorption kinetics models from adsorption process of Fe<sub>3</sub>O<sub>4</sub>/SnO<sub>2</sub>/graphene of 5 wt%. The figure shows the Langmuir isotherm is a better fit than the Freundlich isotherm kinetic model, with the value of regression coefficient ( $R^2$ ) was 0.99 and 0.88 for Langmuir isotherm and Freundlich adsorption isotherm model, respectively.

#### 4. Conclusion

The Fe<sub>3</sub>O<sub>4</sub>/SnO<sub>2</sub> nanocomposite and the different weight percentages of graphene (1, 3, 5 wt%) in Fe<sub>3</sub>O<sub>4</sub>/SnO<sub>2</sub>/graphene have been successfully synthesized by using ultrasonic assisted and co-precipitation method, respectively. The structural characterization of the samples was studied by using XRD measurement, which revealed a combination phase from the tetragonal phase of SnO<sub>2</sub> and cubic spinel phase of Fe<sub>3</sub>O<sub>4</sub>. The TGA measurement confirmed the existence of graphene in Fe<sub>3</sub>O<sub>4</sub>/SnO<sub>2</sub>/graphene composite by showing the weight loss at around 400°C which attributes to combustion effect from graphene. The maximum equilibrium adsorption capacity reached Fe<sub>3</sub>O<sub>4</sub>/SnO<sub>2</sub>/graphene of 5wt% with the value of 44.19 mg/g. The maximum adsorption capacity was obtained at the pH value of 13 for Fe<sub>3</sub>O<sub>4</sub>/SnO<sub>2</sub>/graphene of 5 wt% composite. The adsorption process of Fe<sub>3</sub>O<sub>4</sub>/SnO<sub>2</sub>/graphene 5 wt% follows the Langmuir adsorption isotherm model.

#### 5. References

- [1] Zahra Khodami, Alireza Nazamzadeh-Ejhiieh 2015 *Journal of Molecular Catalyst A: Chemical* **409** 59-68
- [2] Sung Phil Kim, Myong Yong Choi, Hyun Chul Choi 2016 *Materials Research Bulletin* **74** 85-89 [3] Lukumoni Borah, Mridusmita Goswami, Prodeep Phukan 2015 *Journal of Environmental Chemical Engineering* **3** 1018-1028
- [4] Jiali Chang, Jianchao Ma, Qingliang Ma, Duoduo Zhang, Nannan Qiao, Mengxiao Hu, Hongzhu Ma 2016 *Applied Clay Science* **119** 132-140
- [5] Wenjuan Wang, Heipeng Zhang, Ling Zhang, Haiqin Wan, Shourong Zheng, Zhaoyi Xu 2015 *Colloids and Surface A: Physicochem. Eng. Aspects* **469** 100-106
- [6] Haomiao Xu, Zan Qu, Songjian Zhao, Dongting Yue, Wenjun Huang, Naiqiang Yan 2016 *Chemical Engineering Journal* **292** 123-129
- [7] Zhibin Wu, Hua Zhong, Xingzhong Yuan, Hou Wang, Lele Wang, Xiaohong Chen, Guangmin Zeng, Yan Wu 2014 *Water Research* **67** 330-344
- [8] Huan Wang, Haihuan Gao, Mingxi Chen, Xiaoyang Xu, Xuefang Wang, Cheng Pan, Jianping Gao 2016 *Applied Surface Science* **360** 840-848
- [9] Cao C, Xiao L, Chen C, Shi X, Cao Q, Gao L 2014 *Powder Technology* **260** 90-97
- [10] Dalvand A, Nabizadeh R, Ganjali M R, Khoobi M, Nazmara S, Mahvi A H 2016 *Journal of Magnetism and Magnetic Materials* **404** 179-189
- [11] Taufik A, Susanto I K, Saleh R 2015 *Materials Science Forum* **827** 37-42
- [12] Yue Li, Yanqun Guo, Ruiqin Tan, Ping Cui, Yong Li, Weijie Song 2009 *Materials Letters* **63** 2085-2088
- [13] Lihua Hu, Zhongping Yang, Limei Cui, Yan Li, Huu Hao Ngo, Yaoguang Wang, Qin Wei, Hongmin Ma, Liangguo Yan, Bin Du 2016 *Chemical Engineering Journal* **287** 545-556
- [14] Loryuenyong V, Totepvimarn K, Eimburanaprat P, Boonchompoo W and Buasri A 2013 *Advances in Material Science and Engineering* **2013** 923403

- [15] Singh D, Verma S, Gautam R K, Krishna V 2015 *Journal of Environmental Chemical Engineering* **3** 2161-2171
- [16] Linson Lonappan, Tarek Rouissi, Ratul Kumar Das, Satinder K Brar, Antonio Avalos Ramirez, Mausam Verma, Rao Y Surampalli, Valero J R 2016 *Water Management* **49** 537-544
- [17] Saleh R, Djaja N F 2014 *Spectrochim. Acta Part A* **130** 581-590